

# Validation of Virtual Prototyping through Test Measurements on Physical Prototype

Todor Todorov<sup>1, a)</sup> Krasimira Bineva<sup>1, 2, b)</sup> Konstantin Kamberov<sup>1, 3, c)</sup>

<sup>1</sup> Lab. "CAD/CAM/CAE in Industry", FIT, Technical University of Sofia line Sofia, Bulgaria

a) [todortodorov@tu-sofia.bg](mailto:todortodorov@tu-sofia.bg)

b) [krdimova@tu-sofia.bg](mailto:krdimova@tu-sofia.bg)

c) [kkamberov@tu-sofia.bg](mailto:kkamberov@tu-sofia.bg)

**Abstract:** The work presented demonstrate a structural rigidity analysis under steady-state static loads. Separate analysis is performed as to reproduce physical measurement conditions and results. Assessment of accuracy and precision between virtual prototype and physical test product is made by measurement over real part for simulation verification. Defined are examined load case results by max equivalent stress and deformation values based on boundary conditions.

## INTRODUCTION

All the forces in the real world act dynamically on structures. Since dynamic loads are extremely difficult to handle in analysis and design, static loads are usually utilized with dynamic factors. Generally, the dynamic factors are determined from design codes or experience. [1]

Static loading is a load that doesn't change over time. They tend to be better defined and require less of a safety factor on them than dynamic loading. It is also common practice to take a snap shot in time of a mechanical system and assume it is static in order to simplify the analysis process. In many structural codes, the types of loading are split into static, cyclical and incidental or some variation, and indicate a different safety factor for each based on the degree of risk each poses. For instance, a static load on an overhead crane would be the weight of the structure, block, etc., because those never change.

## PROJECT DEFINITION

A front panel design is to be assessed as structural rigidity under steady-state static loads. Its geometry is shown on figure 1 below.

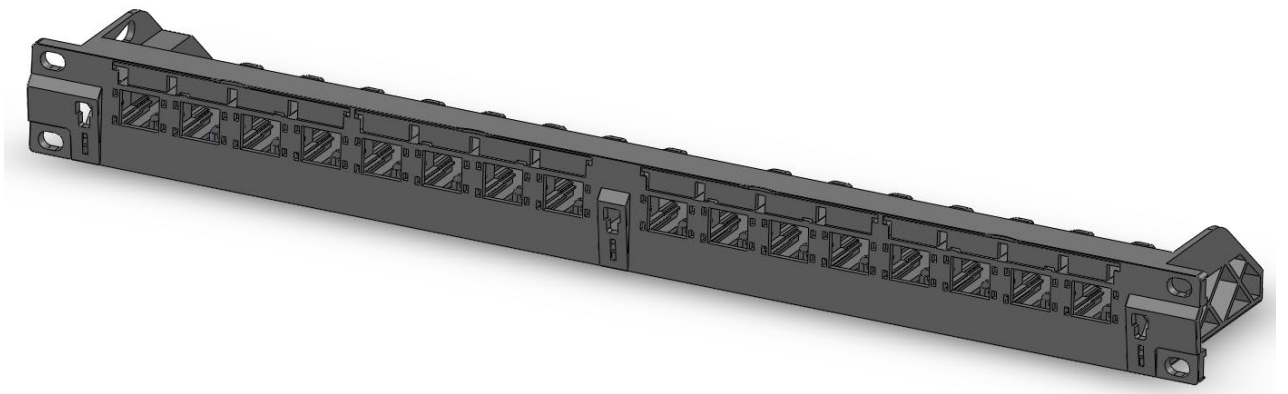


**FIGURE 1.** Examined design of test product

Following load cases of the RDM test panel are examined:

- Applied load of 48N;
- Applied load of 100N (refer to figure 2).

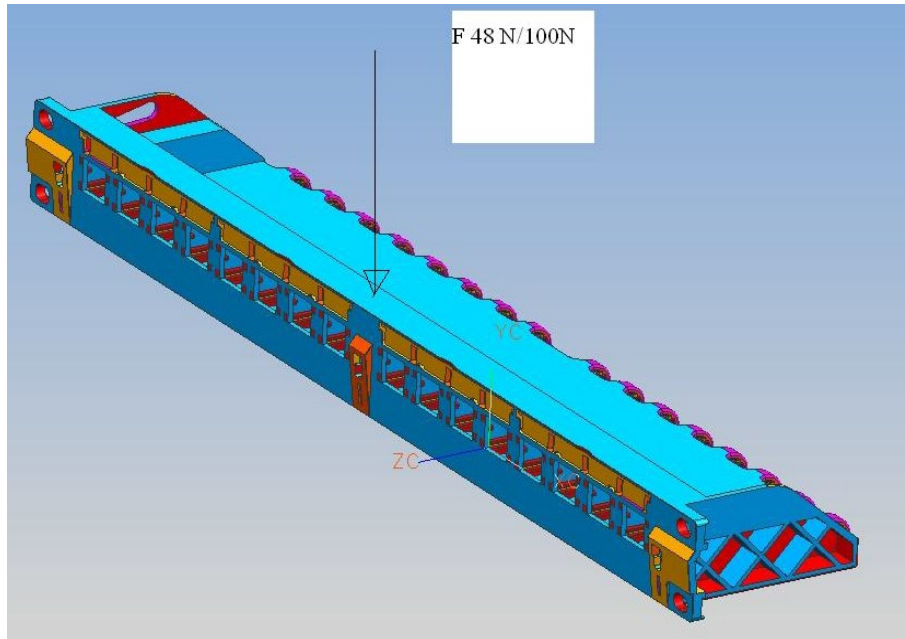


**FIGURE 2.** Load cases specification

Performed analyses results are to be the next major parameters:

- Deformation;
- Equivalent stress.

### **SIMULATION MODEL AND HYPOTHESIS**

There are no simplifications over received geometry model, but additional connecting screws are added to represent more correctly overall examined structures force-deflection behaviour. Used for simulations model are shown in general on figure 3 below. The model is presented as half, because of geometry and loads symmetry, which allows less expensive, but more accurate modelling.

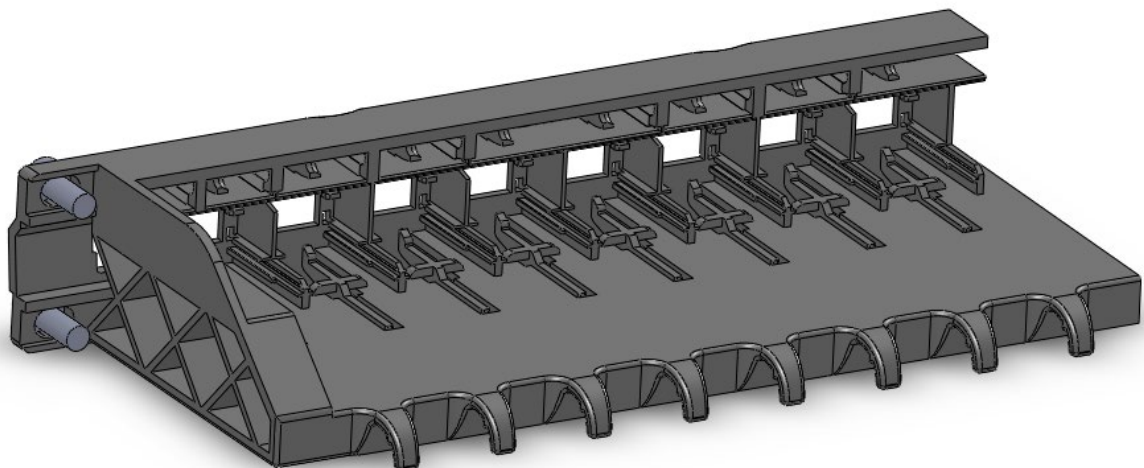


**FIGURE 3.** Geometry model with symmetry

Meshed structure are built, based on the above mentioned geometry model. Examined model contains about 609 000 nodes and 176 000 elements and are shown on figure 4 as to present the density of the mesh.

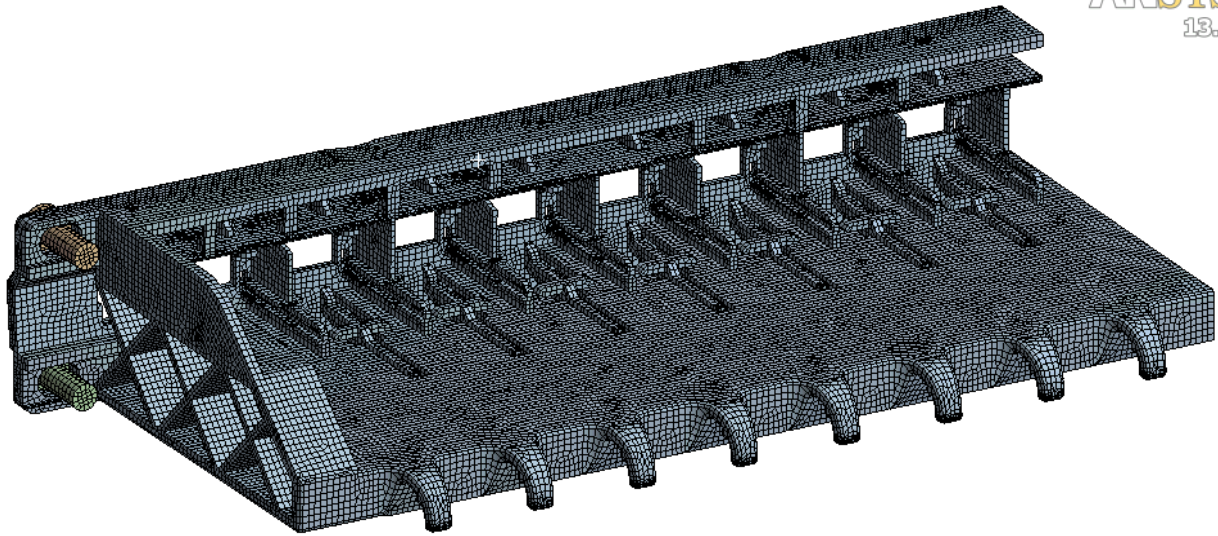


FIGURE 4. Meshed model

All contacts between both modelled parts are presented as of “Bonded” type.

Applied boundary conditions are shown on figure 5 – as constraints and as applied loads. All DOFs are constrained in screw locations and transverse (model axis X) symmetry plane is constrained at “cut” surface. Load, marked as force on the figure below, for load case 1 (LC1) is 48N, and for LC2 – 100N.

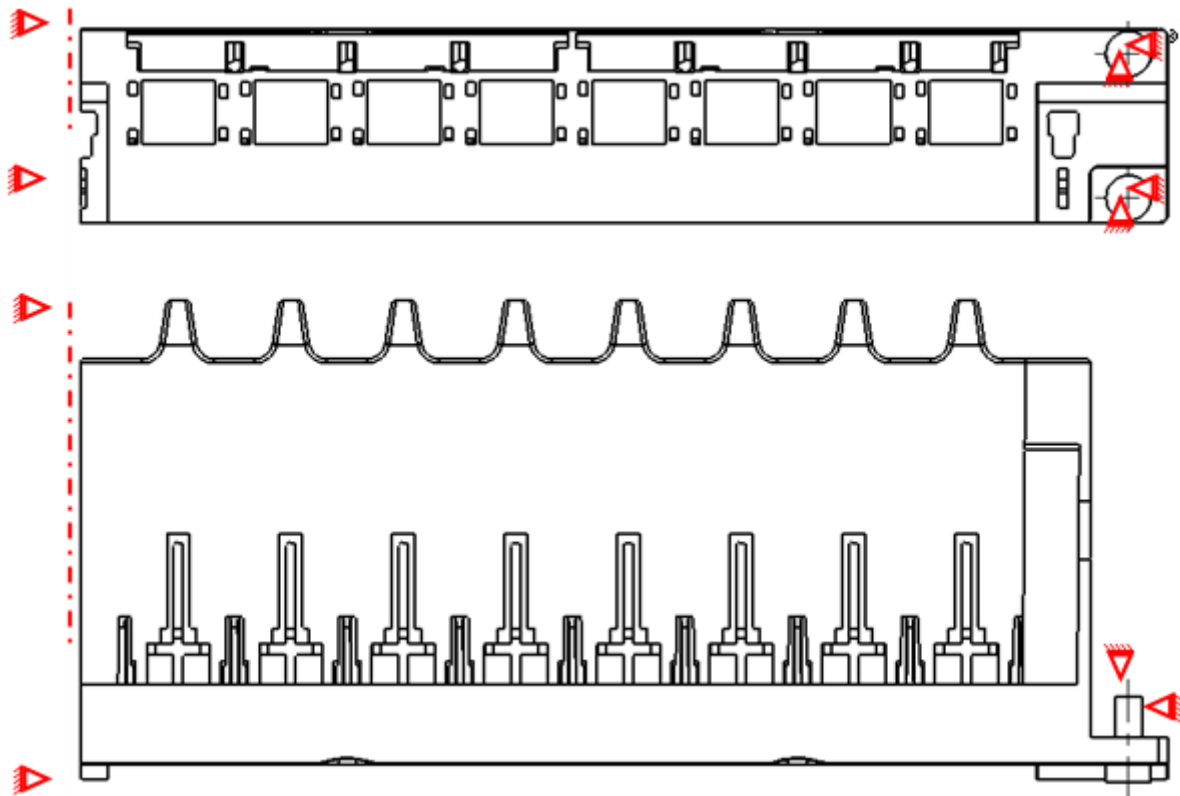
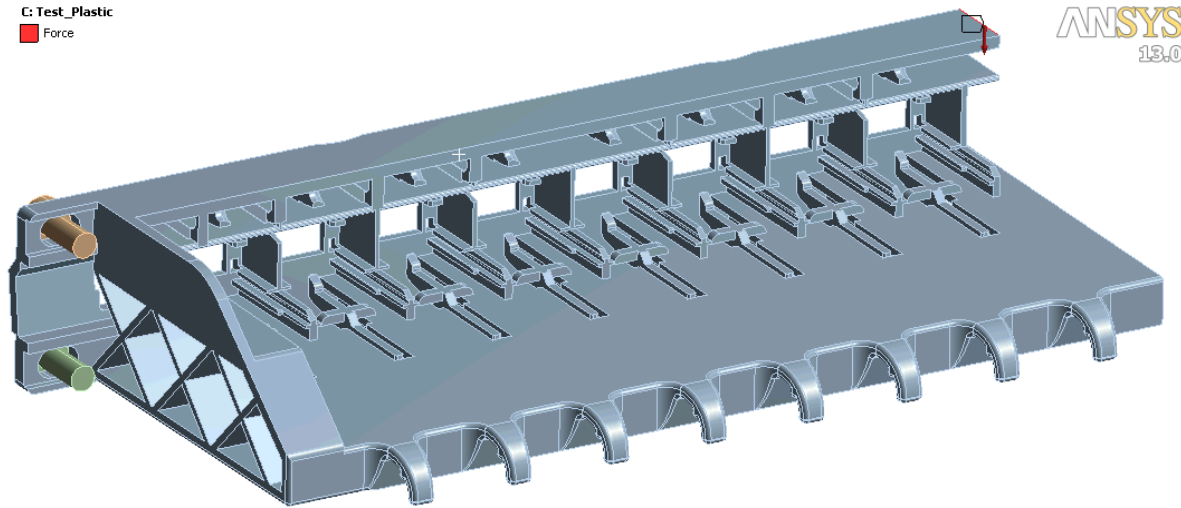


FIGURE 5. Boundary conditions – Constrained DOFs – valid for both load cases



**FIGURE 6.** Boundary conditions – Applied force on middle edge of the part

Material parameters are based on the document “500R.pdf (for LEXAN 500R), from internet available resources. All major parameters used in subsequent analyses are shown in table 1.

**TABLE 1** Material properties

Parameter	LEXAN 500R
Elasticity modulus, E, GPa	3.4
Poisson's ratio, $\mu$	0.36 <sup>1</sup>
Density, $\rho$ , kg/m <sup>3</sup>	1250
Yield tensile strength, MPa	45
Ultimate tensile strength, MPa	60

## SIMULATION RESULTS

Obtained results are reported grouped by load cases. Maximal deformation and equivalent stress values are examined, according to specified requirements. Each model results are presented by its total deformation and equivalent (von Mises) distribution fields on subsequent figures.

- Load case 1 – 48N applied on middle edge

Next figures present results for loads according to specification of load case 1

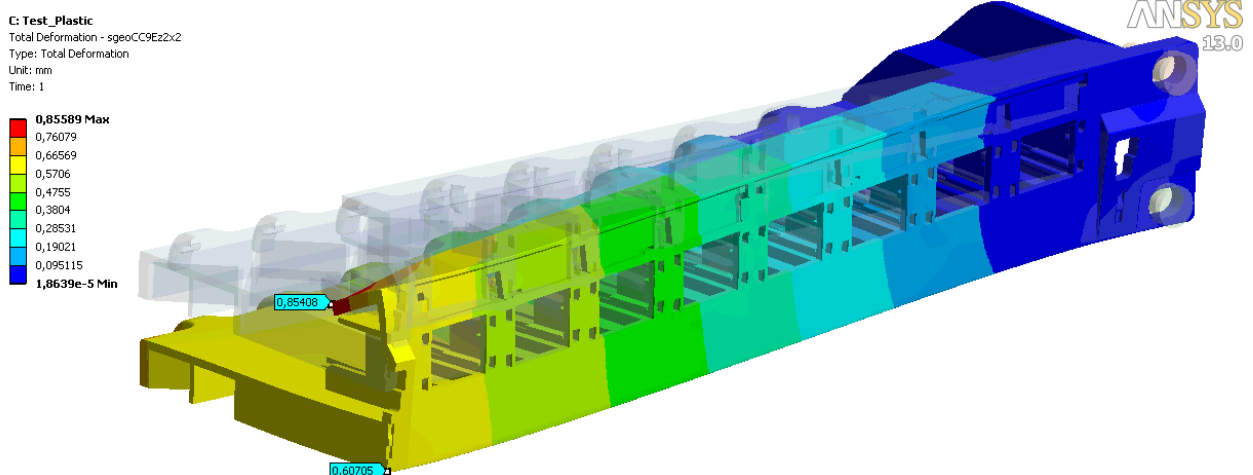


**FIGURE 7.** LC1 – 48N applied on middle edge. Total deformation field, mm. Local deformation: 0.86mm. Deformation of vertical bar: 0.6mm. Scale – 30:1

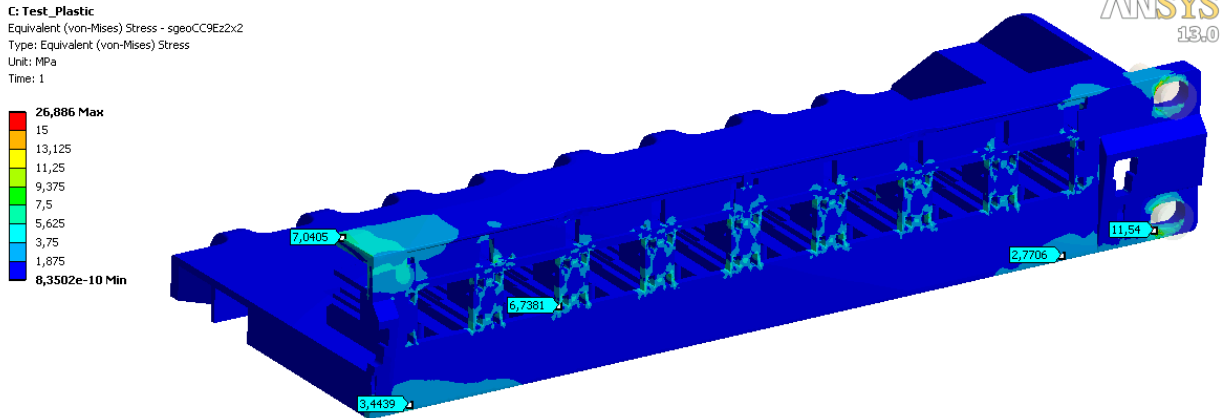


FIGURE 8. LC1 – 48N applied on middle edge. Equivalent (von Mises) stress field, mm. Max value: 11.5MPa. Scale – 1:1

- Load case 2 – 100N applied on middle edge

Results for load case 2 are presented on figures 9 and 10 – again by distributions of equivalent stresses and of total deformation.

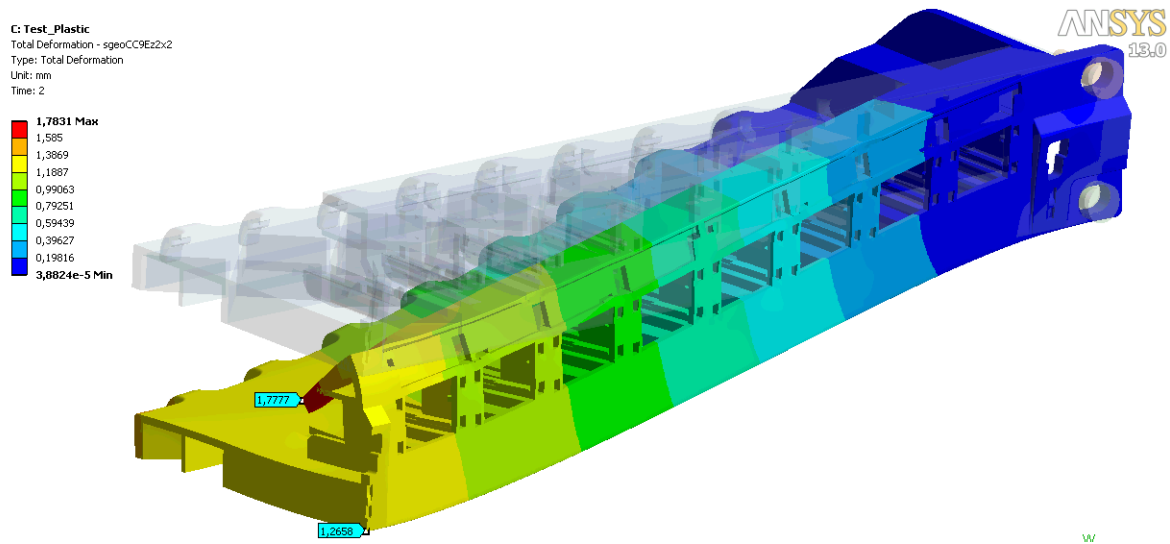


FIGURE 9. LC2 – 100N applied on middle edge. Total deformation field, mm. Local deformation: 1.78mm. Deformation of vertical bar: 1.27mm. Scale – 30:1

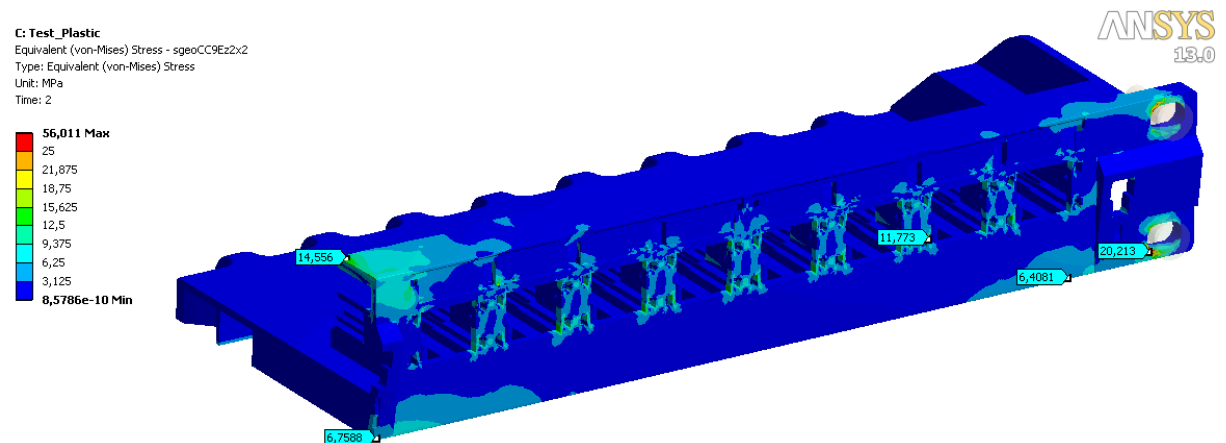
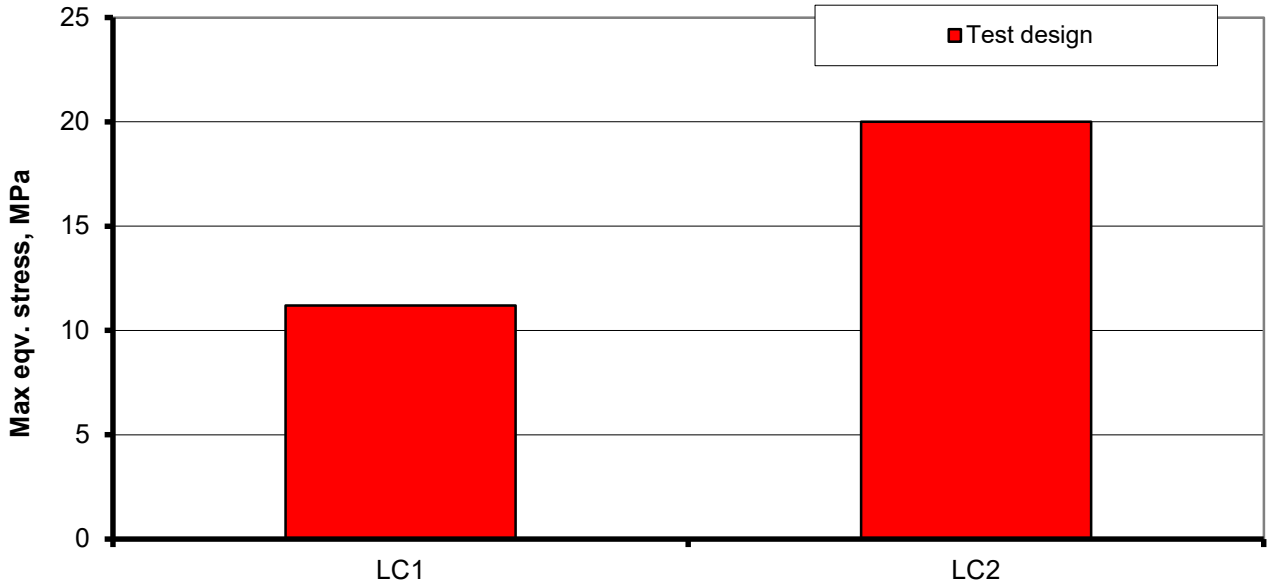


FIGURE 10. LC2 – 100N applied on middle edge. Equivalent (von Mises) stress field, mm. Max value: 20MPa. Scale – 1:1

Simulations results analysis leads to the next several major comments:

- All results are compared as deformations on figure 15, and as equivalent stresses – on figure 10 – for better overview:



**FIGURE 11.** Comparison between examined load cases by max equivalent (von Mises) stress values

- Maximal deformation is 1.27mm under vertical front bar and – 1.78mm local deformation of flat transverse wall;
- There are no critical stresses as maximum value is about 20mpa and yield strength – 45MPa.

### **NUMERICAL SIMULATION AND PHYSICAL MEASUREMENT**

Separate analysis is performed as to reproduce physical measurement conditions and results. The target is to compare results from numerical simulation against physical measurement. Both simulation hypothesis and material properties are expected to be validated.

- Numerical simulation

Applied boundary conditions are shown on figure 12 – as constraints and as applied loads. All DOFs are constrained in screw locations and transverse (model axis X) symmetry plane is constrained at “cut” surface. Load, marked as force on the figure below is equal to 3.530kg, or 34.62N. Half value is applied on simulation model as it is symmetric.

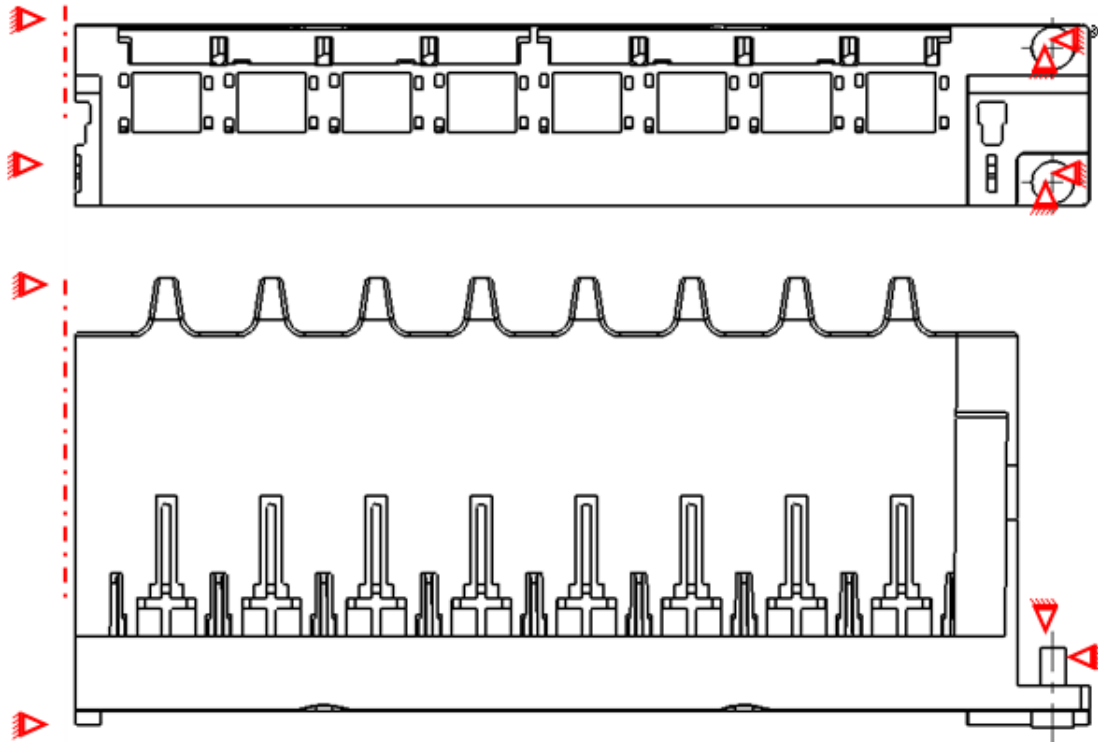


FIGURE 12. Constrained DOFs – valid for both load cases

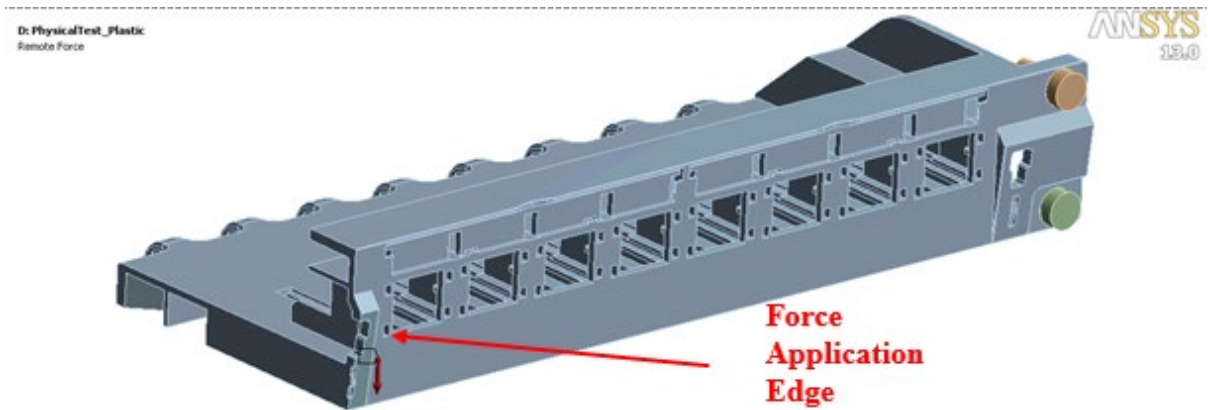


FIGURE 13. Applied force on the edge of first frontal side cut

Deformation is the major result, used for verification.

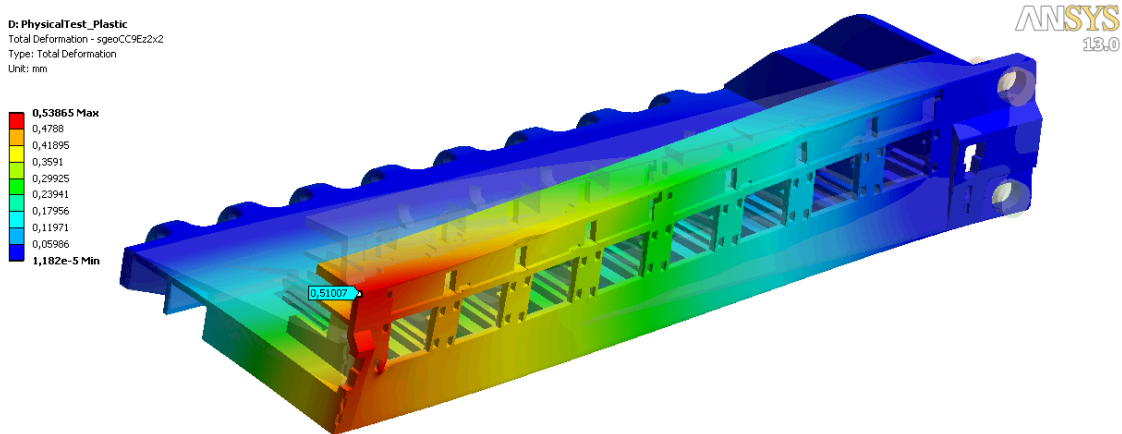


FIGURE 14. Simulation verification. Total deformation field, mm. Local deformation: 0.51mm. Scale – 30:1

- Physical testing and measurements

Measurement method needs to correspond to the performed numerical simulation by FEM. Thus, the next scheme, shown on figure 14 below, is provided for test measurements. It involves measurement by a mechanical comparator of the directional displacement under the point of force application. This point is considered to be on the top of horizontal bar. Bending force is generated by hanging on hook a preliminary measured weight (dead load). This requires definitively exact orientation of the examined sample towards gravity.

Test data is based over 10 measurements as to determine mean value that to be used further. Each measurement starts without applied load – for initialisation of the mechanical comparator. Next step is to apply the load by hooking on measured weight. Mechanical comparator value is recorded down.

Both measured load and displacement are used for subsequent analysis and verification – with direct comparison to results from performed simulation.

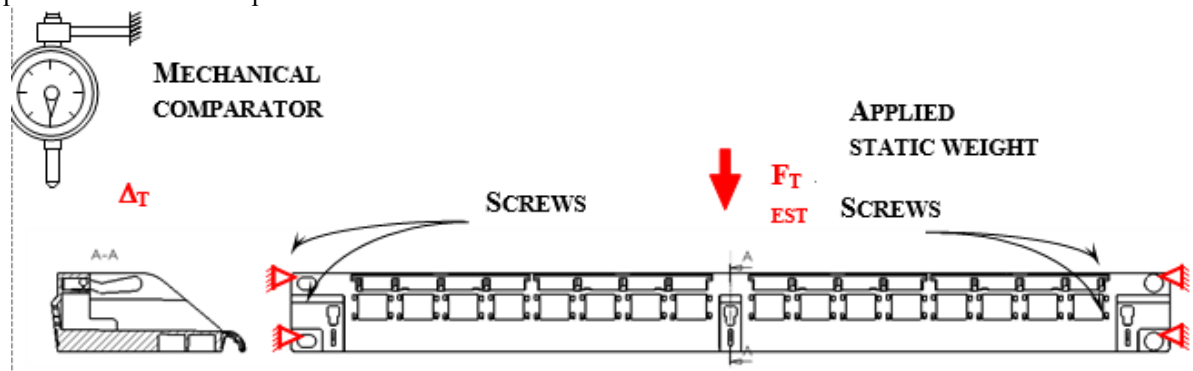
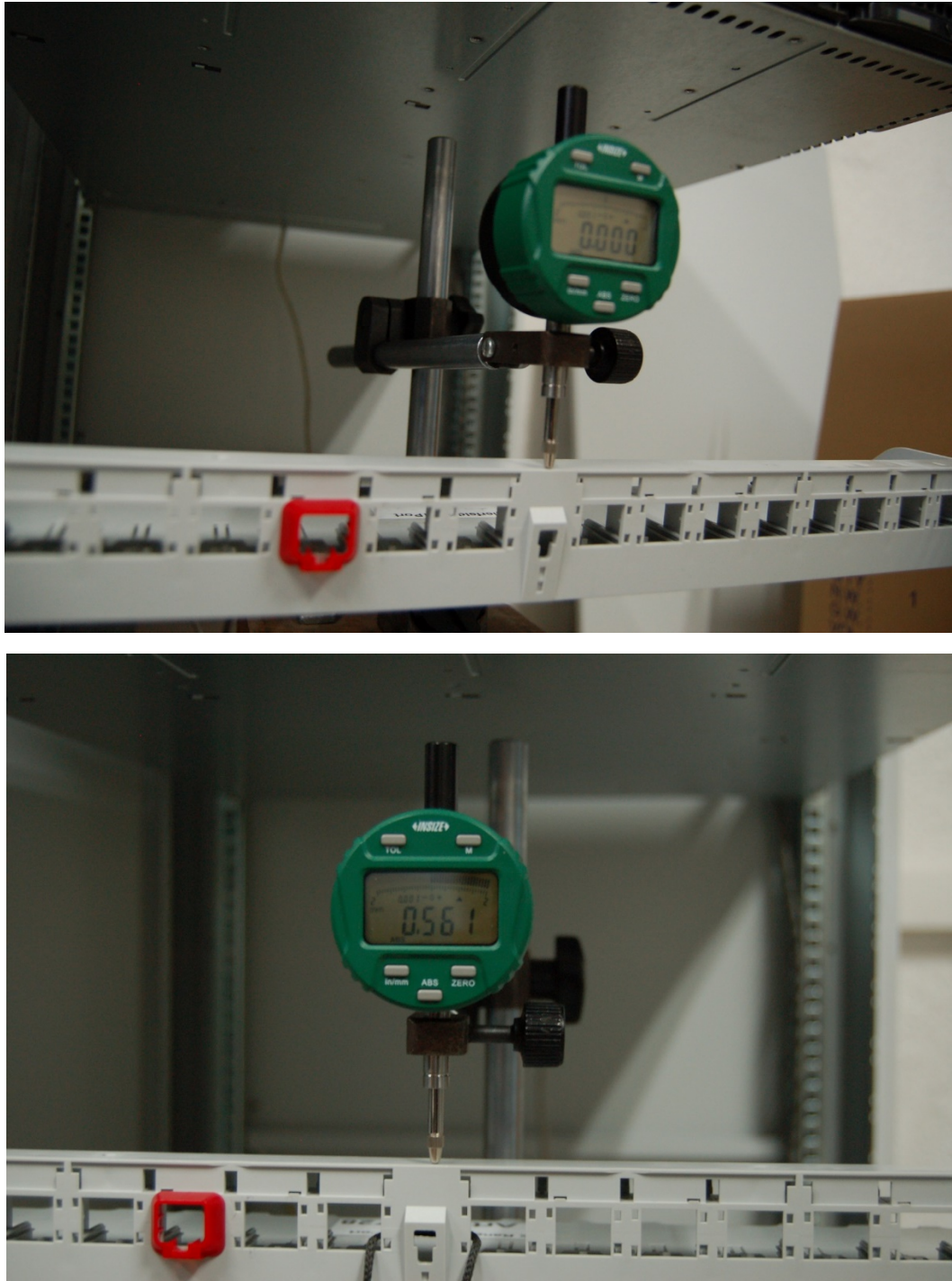


FIGURE 15. Simulation verification. Examined existing part – measurement method

Performed measurement over real product is demonstrated through photos on the next figure.





**FIGURE 16.** Simulation verification. Measurement over real part

Measured displacement over the comparator is after removing the sample weight and elastic “spring back” of the clip in its nominal position. Measured values over 10 separate tests are shown in table 2 below.

<b>TABLE 2</b> Measured data	
<b>Test #</b>	<b>RELATIVE DISPLACEMENT, MM</b>
1	0.561
2	0.565
3	0.561
4	0.563
5	0.571
6	0.573

7	0.558
8	0.555
9	0.560
10	0.556
<b>Average</b>	<b>0.562</b>

- Relative comparison

The comparison is performed based on applied force and measured/calculated deformation only. This is summarized in table 3 below and graphically displayed on figure 17.

Parameter	FE model	Physical part measurement
Bending force, $F_b$ , N	34.62	34.62
Deformation, $\Delta$ , mm	0.51	0.562
Bending stiffness, $k$ , N/mm	67.88	61.6
Relative comparison		
Bending force	100	100
Deformation	90.7	100

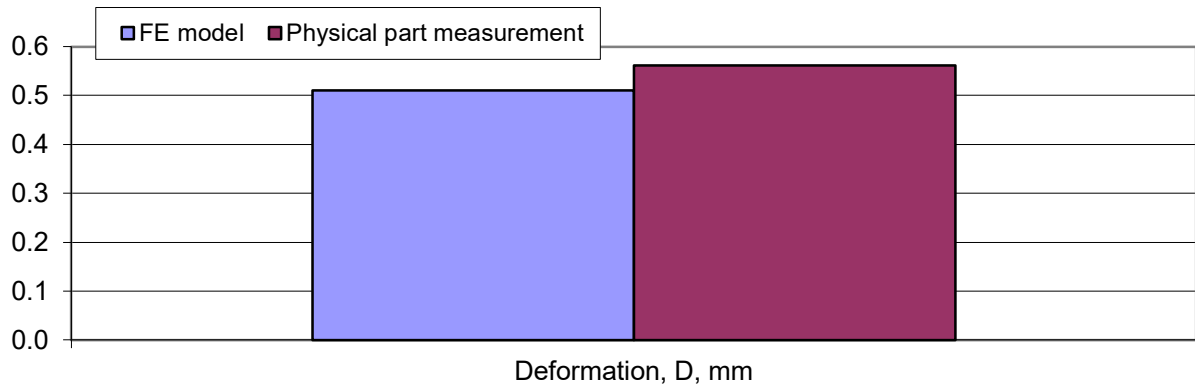


**FIGURE 17.** Simulation verification. Comparison @ work load by simulation and measurement over physical prototype results

## CONCLUSION

After separate analysis is performed, the measurements between virtual and physical prototype shows similar behavior. This study shows a high matching between virtual and physical models, as well as this example could be used in practice to predict process issues of design components.

## ACKNOWLEDGMENT

„This study is financed by the European Union-NextGenerationEU, through the National Recovery and Resilience Plan of the Republic of Bulgaria, project № BG-RRP-2.004-0005”.

## REFERENCES

- [1] A. El Saddik, "Digital Twins: The Convergence of Multimedia Technologies," IEEE MultiMedia, vol. 25, no. 2, pp. 87-92, 2018.
- [2] В. Гълъбов, Я. Софронов and А. Милев, "Синтез на основния механизъм на робот екстрактор на отливки," Механика на машините, no. 97, pp. 3-8, 2012.
- [3] LC-Insights LLC, "Virtually Prototyping with Digital Twins > Lifecycle Insights," 2016. [Online]. Available: <http://www.lifecycleinsights.com/tech-guide/virtually-prototyping-with-digital-twins/>. [Accessed 2017].

- [4] В. Гълъбов, Я. Софронов and А. Милев, "Определяне на предавателните функции на механизми за ориентация на крайния ефектор на шестзвенни Q-манипулатори," *Механика на машините*, no. 97, pp. 15-19, 2012.
- [5] B. N. Zlatev, G. D. Todorov and K. D. Dimova, "Optimization of the efficiency of a Kinetic Uninterruptible Power Supply with a Flywheel Mass Accumulator," in *XXIX INTERNATIONAL SCIENTIFIC AND TECHNICAL CONFERENCE AUTOMATION OF DISCRETE PRODUCTION ENGINEERING*, Sozopol, 2020.
- [6] G. D. Todorov, K. H. Kamberov and B. N. Zlatev, "Exploration of the advantages and an algorithm for the implementation of the digital twin concept," in *XXIX International Scientific Symposium Metrology and Metrology Assurance*, Sozopol, 2019.